

Received:
25 June 2018Revised:
23 November 2018Accepted:
01 January 2019<https://doi.org/10.1259/bjr.20180562>

Cite this article as:

Rado SD, Lorbeer R, Gatidis S, Machann J, Storz C, Nikolaou K, et al. MRI-based assessment and characterization of epicardial and paracardial fat depots in the context of impaired glucose metabolism and subclinical left-ventricular alterations. *Br J Radiol* 2019; **92**: 20180562.

FULL PAPER

MRI-based assessment and characterization of epicardial and paracardial fat depots in the context of impaired glucose metabolism and subclinical left-ventricular alterations

¹SOPHIA D RADO, MD, ²ROBERTO LORBEER, PhD, ¹SERGIOS GATIDIS, MD, ^{3,4,5}JÜRGEN MACHANN, PhD, ¹CORINNA STORZ, MD, ¹KONSTANTIN NIKOLAOU, MD, ^{5,6}WOLFGANG RATHMANN, MD, MSPH, ⁷UDO HOFFMANN, MD, ^{8,9,10}ANNETTE PETERS, PhD, ^{1,8,11}FABIAN BAMBERG, MD, MPH and ^{11,12}CHRISTOPHER L SCHLETT, MD, MPH

¹Department of Diagnostic and Interventional Radiology, University Hospital Tuebingen, Tuebingen, Germany

²Department of Radiology, Ludwig-Maximilian-University Hospital, Munich, Germany

³Department of Diagnostic and Interventional Radiology, Section on Experimental Radiology, University Hospital Tuebingen, Tuebingen, Germany

⁴Institute for Diabetes Research and Metabolic Diseases (IDM) of the Helmholtz Center Munich at the University of Tuebingen, Tuebingen, Germany

⁵German Center for Diabetes Research (DZD), Neuherberg, Germany

⁶Institute for Biometrics and Epidemiology, German Diabetes Center, Leibniz Center for Diabetes Research at Heinrich Heine University Düsseldorf, Düsseldorf, Germany

⁷Department of Radiology, Massachusetts General Hospital, Harvard Medical School, Boston, MA, USA

⁸German Center for Cardiovascular Disease Research (DZHK e.V.), Munich, Germany

⁹Institute for Cardiovascular Prevention, Ludwig-Maximilian-University-Hospital, Munich, Germany

¹⁰Institute of Epidemiology II, Helmholtz Zentrum München, German Research Center for Environmental Health, Neuherberg, Germany

¹¹Department of Radiology, University Hospital Freiburg, Freiburg, Germany

¹²Department of Radiology, Diagnostic and Interventional Radiology, University of Heidelberg, Heidelberg, Germany

Address correspondence to: Christopher L Schlett

E-mail: Christopher.Schlett@post.harvard.edu

Objective: To analyze the associations between epicardial and paracardial fat and impaired glucose tolerance as well as left ventricular (LV) alterations.

Methods: 400 subjects underwent 3 T MRI and fat depots were delineated in the four chamber-view of the steady-state free precession cine sequence (repetition time: 29.97 ms; echo time 1.46 ms). LV parameters were also derived from MRI. Oral glucose tolerance tests were performed.

Results: Epi- and paracardial fat was derived in 372 (93%) subjects (220 healthy controls, 100 persons with prediabetes, 52 with diabetes). Epi- and paracardial fat increased from normal glucose tolerance (NGT) to prediabetes and diabetes (7.7 vs 9.2 vs 10.3 cm² and 14.3 vs 20.3 vs 27.4 cm², respectively; all $p < 0.001$). However, the association between impaired glucose metabolism and cardiac fat attenuated after adjustment,

mainly confounded by visceral adipose tissue (VAT). 93 subjects (27%) had LV impairment, defined as late gadolinium enhancement, ejection fraction < 55% or LV concentricity index > 1.3 g ml⁻¹. Mean epicardial fat was higher in subjects with LV impairment (11.0 vs 8.1 cm², $p < 0.001$). This association remained independent after adjustment for traditional risk factors and VAT [β : 1.13 (0.22; 2.03), $p = 0.02$].

Conclusion: Although epicardial and paracardial fat are increased in prediabetes and diabetes, the association is mostly confounded by VAT. Epicardial fat is independently associated with subclinical LV impairment in subjects without known cardiovascular disease.

Advances in knowledge: This study contributes to the picture of epicardial fat as a pathogenic local fat depot that is independently associated with MR-derived markers of left ventricular alterations.

INTRODUCTION

Several studies have investigated distinct local fat depots, since these show stronger associations with traditional risk factors and/or cardiovascular disease as compared to

anthropometric measurements of obesity;^{1,2} most promising evidence has been reported for assessing abdominal visceral adipose tissue (VAT)¹ and epicardial fat,^{3,4} which is located within the visceral layer of the pericardium.

Epicardial fat shows endocrine activities,^{5,6} is considered to provide the heart with energy metabolites,⁷ and to protect the heart from hypothermia.⁸ Given the anatomic close relationship of epicardial fat with the left ventricle (LV) and the coronary arteries, a local toxic effect on the heart has been postulated,^{4,9} given the associations to coronary artery disease,^{10,11} atrial fibrillation^{12,13} and impairment of cardiac function.¹⁴ In contrast, the role of paracardial fat, the fat compartment outside the parietal pericardium, is not fully understood.^{3,4,15}

Beside the associations to cardiovascular disease, local fat depots have been studied in comparison to impaired glucose tolerance. Briefly, VAT—as a relatively large fat depot—has shown associations to diabetes, and also prediabetes as a metabolic disorder.^{16,17} In a study by Arpacı et al including 64 prediabetic and 30 healthy subjects, epicardial fat appears to be increased in subjects with prediabetes in comparison to healthy controls.¹⁸ Song et al showed that epicardial fat was increased in subjects with Type 2 diabetes mellitus and obesity.¹⁹ Thus, overall broad evidence is limited so far.

Impaired glucose metabolism has shown to be associated with early structural LV changes.^{20,21} It is known for many years, that diabetes is a major risk factor for the development of cardiovascular disease.²² MRI of the heart is a well-established diagnostic modality for structural heart disease including the assessment of LV volume/mass as well as LV function, but also coronary artery disease, using late gadolinium enhancement (LGE) as a marker of myocardial scar. However, MRI has rarely been used for the assessment of epicardial fat in study cohort settings, which traditionally employ either ultrasound-based echocardiography²³ or CT.^{3,4,24} Nevertheless, MRI—particular whole-body MRI—is more and more frequently applied in epidemiological cohort studies like the German National Cohort or UK Biobank.²⁵ In this context, the possibility of radiation-free assessment of the cardiac fat depots by MRI becomes feasible.

Thus, our aim was to assess epi- and paracardial fat as derived from whole-body MRI and to relate it to prediabetes and diabetes in comparison to other measures of obesity including VAT. Furthermore, we aimed to assess the association of MR-derived epi- and paracardial fat with subclinical LV impairment in subjects without known clinical history of cardiovascular disease.

METHODS AND MATERIALS

Study population and design

The KORA (“Kooperative Gesundheitsforschung in der Region Augsburg”—Cooperative Health Research in the Region of Augsburg) study has emerged as a follow-up of the MONICA study²⁶ and is a longitudinal, population-based cohort study. Within a follow-up cohort (KORA FF4 cohort, 2013–2014), a nested case–control study focusing on whole-body MRI with a 3 T MR scanner (Magnetom Skyra, Siemens Healthineers, Erlangen, Germany) was implemented including participants with diabetes, prediabetes and normal glucose tolerance. Only subjects without pre-existing cardiovascular conditions such as myocardial infarction, stroke, peripheral artery disease or

coronary intervention were recruited to undergo imaging. Further inclusion and exclusion criteria have been described elsewhere.²⁰

The study was approved by the institutional review board of the Medical Faculty of the Ludwig-Maximilians University Munich, Germany, and all research was conducted in accordance with the Declaration of Helsinki. Prior to undergoing the MRI exams, informed written consent was collected from each participant.

Impaired glucose tolerance and other clinical covariables

The health assessment including the collection of covariables either from interviews, laboratory work or physical exams was conducted in a uniform fashion at the KORA study center between 2013 and 2014 and has been described in detail elsewhere.^{20,26} All subjects without history of diabetes underwent a fasting glucose test and an oral glucose tolerance test (OGTT). Reference values provided by the World Health Organization (Prediabetes is defined as either impaired glucose tolerance: normal fasting glucose concentration and a 2 h serum glucose concentration between 140 and 200 mg dl⁻¹ and/or impaired fasting glucose, with fasting glucose levels between 110 and 125 mg dl⁻¹ and a normal 2 h serum glucose concentration. Diabetes is defined as blood serum glucose ≥ 200 mg dl⁻¹ and/or fasting serum glucose levels > 125 mg dl⁻¹) were employed to classify subjects as either having diabetes, prediabetes or normal glucose tolerance.²⁷ The final sample did not include any subjects with Type 1 diabetes.

Body mass index (BMI) was calculated as body weight (kg) divided by body height squared (m²). Hypertension was defined as systolic/diastolic blood pressure $\geq 140/90$ mmHg or the regular intake of antihypertensive medication under the awareness of suffering from hypertension. Antihypertensive medication was defined according to recent guidelines, lipid-lowering medication included lipid-lowering drugs such as statins or fibrates and antithrombotic medication included anticoagulants as well as antiplatelet medication.²⁰ Information about smoking, alcohol intake and physical activity was obtained from interviews. Cholesterol and triglyceride values were measured in fasting blood samples.²⁸

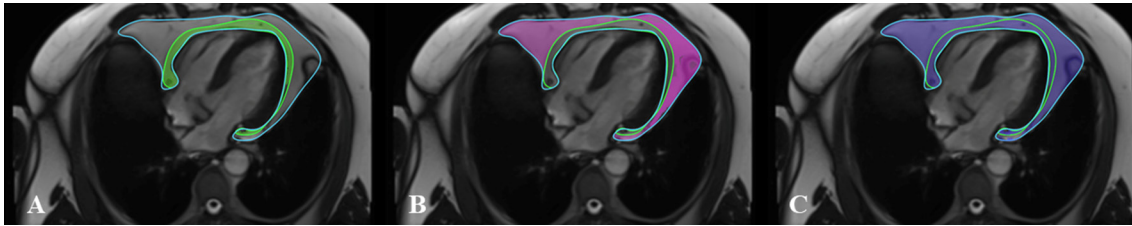
MRI and analysis

The complete and detailed study protocol of the whole-body MRI has been described elsewhere.²⁰

Cardiac fat

The SSFP (steady-state free precession) cine sequence of the heart in the long axis, 4-chamber view was performed as part of the standard study protocol with the following parameters: Time-to-echo (TE) 1.46 ms, time-to-repetition (TR) 29.97 ms, flip angle 63°, matrix 240 × 160, field of view (FOV) 297 × 360 mm, slice thickness 8 mm. The location of the different fat depots in relation to the heart is depicted in Figure 1. The epicardial and pericardial fat compartments were manually delineated in the maximal systole and maximal diastole in an openly available software (OsiriX Lite, Pixmeo, Bernex, Switzerland). Small

Figure 1. Definition of the different fat depots surrounding the human heart on the 4-chamber view long-axis SSFP sequence. The area shaded in green depicts epicardial fat (A), the area shaded in purple depicts paracardial fat (B) and the area shaded in blue depicts pericardial fat (epicardial + paracardial fat) (C). In this study, epicardial (A) and pericardial fat (C) were measured and the amount of paracardial fat (B) was calculated. SSFP, steady-state free precession.



structures embedded in the fat depots such as the coronary arteries, were not segmented separately (Figure 2). Data were recorded as an area in centimeter squared [cm^2]. The amount of paracardial fat was calculated by subtracting the amount of epicardial fat from pericardial fat.

The cardiac fat depots were assessed in end-systole and end-diastole. $\text{ICC}_{\text{intrareader}}$ was 0.918 and 0.844 for epicardial fat in systole and diastole, and 0.985 and 0.979 for pericardial fat in systole and diastole, respectively. $\text{ICC}_{\text{interreader}}$ was 0.884 and 0.765 for epicardial fat in systole and diastole, and 0.927 and 0.888 for pericardial fat in systole and diastole. Due to better intra- and inter-reader reproducibility, all analysis were restricted to the systolic measurements.

MR-based LV assessment

Cardiac parameters regarding function and morphology including end-diastolic volume (EDV), end-systolic volume (ESV), myocardial mass, and ejection fraction (EF) were derived from the cine SSFP sequences in the short axis (10 sl) with the following parameters: TE 1.46 ms, TR 29.97 ms, matrix 240×160 , FOV 297×360 mm, slice thickness 8 mm, flip angle 62° . The endo- and epicardial contours were delineated semi-automatically using a dedicated software (cvi42, Circle Cardiovascular Imaging, Calgary, Canada).

The left-ventricular concentricity index (LVCI) was calculated as LV myocardial mass divided by LV-EDV and values $> 1.3 \text{ g ml}^{-1}$ were considered pathological.²⁹

Data for late gadolinium enhancement (LGE) were derived from FLASH (Fast Low Angle Shot) short axis and a 4-chamber view and were manually analyzed by two readers in a consensus reading. Subendocardial, midmyocardial and epicardial LGE was differentiated.

All data analyses were conducted blinded to the subjects' identities and health status.

Visceral/subcutaneous adipose tissue

A coronal dual-echo DIXON VIBE (Volumetric Interpolated Breath-hold Examination) sequence of the abdomen was performed with the following parameters: TE 1.26; 2.49 ms, TR 4.06 ms, flip angle 9° , matrix 256×256 , FOV 488×716 mm, slice thickness 1.7 mm. Images were acquired within a single breath-hold. From those, fat selective images were automatically calculated.

The amount of VAT/SAT was semi-automatically determined by employing an algorithm based on fuzzy-clustering³⁰ and modified for fat selective VIBE images as described by Fallah et al.³¹

Figure 2. MRI-based assessment of the cardiac fat depots in the systole (A) and diastole (B). The green line depicts the epicardial and the blue line the pericardial fat compartment. The amount of paracardial fat was calculated as "paracardial fat, =pericardial fat-epicardial fat". Ao, aorta descendens; LV, left ventricle.

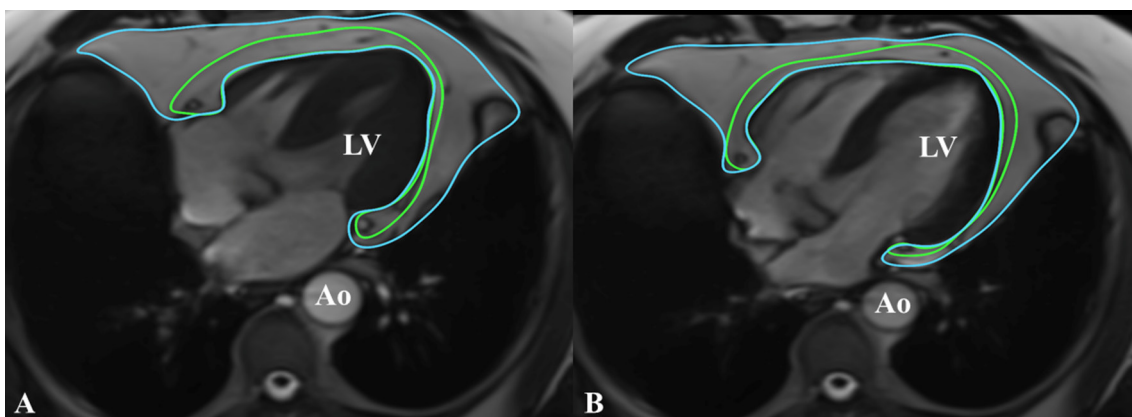
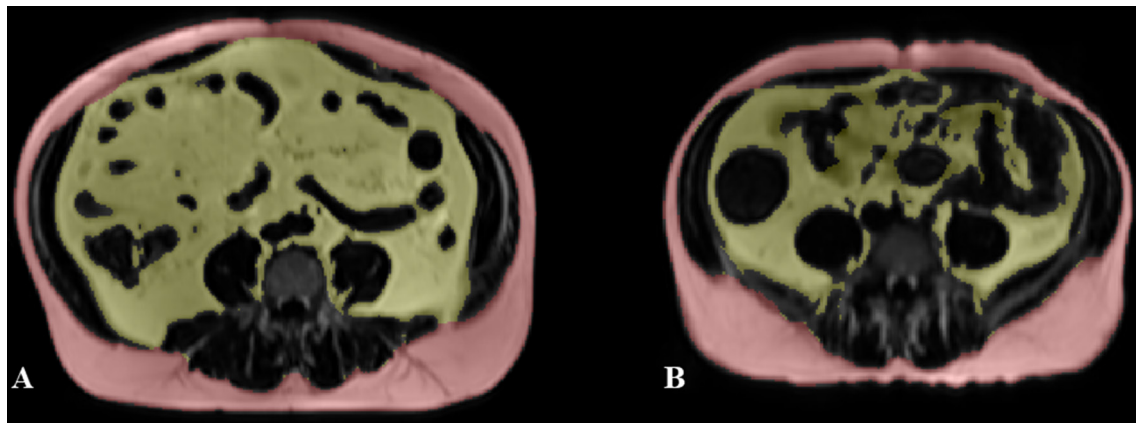


Figure 3. VAT (yellow) and SAT (red) assessment in the abdominal cavity. Axial slices at the umbilical level recorded from a 62-year-old male subject with a high VAT-volume of 12.9l (A) and a 63-year-old male subject with less VAT (4.5 l) (B). Red, subcutaneous adipose tissue (SAT); yellow, visceral adipose tissue (VAT).



In brief, axial fat-selective images (slice thickness 5 mm) were reconstructed from coronal acquired images (Figure 3). VAT in the abdominal cavity was extracted from the total adipose tissue matrix using a three-dimensional statistical shape model, consisting of a geometrical model and a local appearance model. The volume of VAT was quantified from the femoral heads to the cardiac apex while SAT was measured from the femoral heads to the diaphragm.³²

Hepatic proton density fat fraction ($PDFF_{\text{hepatic}}$)

A multiecho VIBE sequence of the upper abdomen was performed with the following parameters: TE 1.23; 2.46; 3.69; 4.92; 6.15; 7.38 ms, TR 8.90 ms, flip angle 4°, FOV 393 × 450 mm. In the calculated PDFF-map, a region of interest (ROI) was manually drawn into the liver parenchyma at the level of the portal vein, thereby avoiding the inclusion of the hilus or large vessels.³³ Data are given in percent.

Statistical analysis

Descriptive demographic, clinical and MRI-derived data are presented separately for glucose tolerance groups as either median [interquartile range (IQR)] for continuous data or number (percentage) for categorical data. Differences among subgroups were tested by Kruskal–Wallis equality of population rank test (continuous data), χ^2 -test (categorical data) or Fisher's exact test (categorical data). Boxplots display graphically the differences of cardiac fat parameters among glucose tolerance groups and between subjects with and without LV impairment.

Since cardiac fat parameters were right skewed distributed, associations between diabetes subgroups and cardiac fat parameters were estimated by median regression analysis using the median as a more valid estimate of the central tendency of the cardiac fat parameters compared to the mean.³⁴ Analyses were stepwise adjusted for potential confounders including age, sex, BMI, hypertension, smoking, triglycerides, LDL-cholesterol, SAT and VAT and β -coefficients with 95% confidence intervals were provided. Associations of cardiovascular risk factors and MR-derived body-fat with cardiac fat parameters were also assessed by multivariable adjusted median regression models. Furthermore,

median regression models for the association between LV impairment and cardiac fat parameters were stepwise adjusted for age, sex, smoking, hypertension, LDL-cholesterol, glucose tolerance status, BMI and VAT.

A two-sided p -value of <0.05 was considered as statistical significant. Data analysis was performed using Stata 14.1 (Stata Corporation, College Station, TX).

RESULTS

Study cohort

Of 400 subjects undergoing whole-body 3 T MRI, 372 were included in the final analysis (93%). Exclusions were predominantly due to artifacts including motion artifacts or misalignment of the FOV for fat assessment. Of the included 372 subjects, 52 had diabetes, 100 had prediabetes and 220 showed normal glucose values (14.0% vs 26.9% vs 59.1%, respectively). Subjects with prediabetes and diabetes were generally older, more often male, and had a more unfavorable cardiometabolic profile than normoglycemic participants. Also, significant differences with regards to the different non-cardiac fat depots including VAT, SAT and $PDFF_{\text{hepatic}}$ were observed (all $p < 0.001$). Detailed demographics are provided in Table 1.

Differences between subjects with impaired glucose tolerance and normoglycemic controls were also observed with regards to most MR-based LV function parameters (Table 2). A total of 93 subjects (27%) had the predefined composite endpoint of presence of LGE, and/or a pathologic LVCI $>1.3 \text{ g ml}^{-1}$, and/or LV ejection fraction $<55\%$; six subjects (1.7%) had more than one of these pathologic LV findings. Thus, a stepwise increase in the presence of the composite endpoint was observed from normal glucose tolerance to prediabetes and diabetes (16.8%, 35.5%, 56.8%, $p < 0.001$; respectively).

Epi- and paracardial fat in the context of impaired glucose metabolism

The median amount of epicardial fat in all study subjects was 8.7 cm^2 (IQR: 5.6–11.2) and of paracardial fat 18.3 cm^2 (IQR:

Table 1. Demographics of the underlying study population

	All subjects N = 372	Normal glucose tolerance N = 220	Prediabetes N = 100	Diabetes N = 52	p-value
Age (years)	57 (49;64)	53 (47;62)	59 (51;66)	63.5 (58;69.5)	<0.001
Male gender (%)	221 (59.4%)	117 (53.2%)	64 (64%)	40 (76.9%)	0.004
BMI (kg m ⁻²)	27.99 (25.16; 31)	26.58 (24.25; 29.01)	29.43 (27.3; 33.82)	30.43 (27.12; 33.09)	<0.001
Hypertension (%)	131 (35.2%)	49 (22.3%)	45 (45%)	37 (71.2%)	<0.001
Antihypertensive medication (%)	97 (26.1%)	39 (17.7%)	32 (32%)	26 (50%)	<0.001
Antithrombotic medication (%)	8 (2.2%)	3 (1.4%)	4 (4%)	1 (1.9%)	0.32
HDL (mg dl ⁻¹)	59.52 (48; 72)	62 (51; 77)	59.26 (49.72; 69.6)	48.16 (40.5; 61.2)	<0.001
LDL (mg dl ⁻¹)	138 (116; 161)	136 (115.5; 162.5)	143.5 (123; 161.5)	130.5 (109.5; 150.5)	0.09
Triglycerides (mg dl ⁻¹)	110.5 (77.28; 162.5)	95.5 (69.5; 129.69)	136.5 (98; 184.62)	177.82 (114.76; 273.09)	<0.001
Lipid lowering medication (%)	42 (11.3%)	15 (6.8%)	9 (9%)	18 (34.6%)	<0.001
SAT (l)	7.41 (5.53; 10.05)	6.75 (5.16; 8.88)	8.65 (6.35; 11.97)	8.65 (6.3; 11.27)	<0.001
VAT (l)	4.23 (2.69; 6.35)	3.14 (1.8; 4.72)	5.44 (3.97; 7.32)	6.88 (5.76; 8.45)	<0.001
PDFF _{hepatic} (%)	4.77 (2.79; 12.21)	3.44 (2.2; 5.9)	11.6 (4.79; 17.93)	15.89 (6.86; 24.13)	<0.001
Smoking status					0.11
Never-smoker	136 (36.6%)	88 (40.0%)	32 (32.0%)	16 (30.8%)	
Ex-smoker	163 (43.8%)	84 (38.2%)	50 (50.0%)	29 (55.8%)	
Current-smoker	73 (19.6%)	48 (21.8%)	18 (18.0%)	7 (13.5%)	

BMI, body mass index; HDL, high-density lipoprotein; LDL, low-density lipoprotein; PDFF, proton-density fat fraction; SAT, subcutaneous adipose tissue; VAT, visceral adipose tissue.

Continuous data are expressed as median (interquartile range) and categorical data as number (percentage). *p* values are from Kruskal-Wallis equality of population rank test (continuous data) or χ^2 -test (categorical data).

11.1–27.3). There was a significant increase in both cardiac fat depots from normal glucose tolerance to prediabetes and diabetes (all *p* < 0.001; [Figure 4](#)). For all subgroups, the epicardial fat depot was smaller than the paracardial fat depot.

Stepwise adjustment of the relation between prediabetes and epicardial fat showed a loss of significance for the prediabetes group upon adjustment for age and gender, while a loss of

significance for the diabetes group was seen upon further adjustment for age, gender and traditional cardiovascular risk factors (excluding BMI; [Table 3](#)). A loss of significance was seen for paracardial fat and prediabetes after adjustment for age, gender and traditional cardiovascular risk factors (excluding BMI). Paracardial fat was associated with diabetes after adjustment for age, gender, traditional cardiovascular risk factors (excluding and including BMI) as well as SAT ([Table 4](#)).

Table 2. Early MRI-based LV parameters in the context of prediabetes and diabetes in the study population

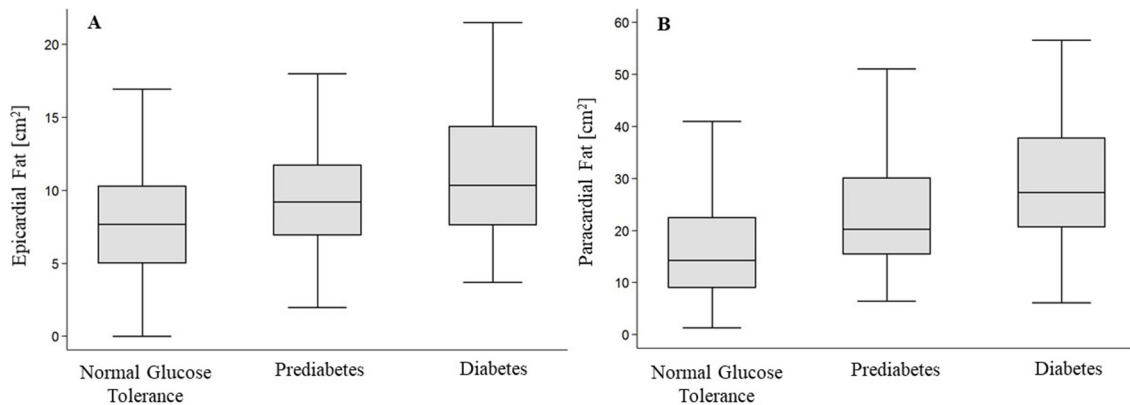
	All subjects N = 345	Normal glucose tolerance N = 208	Prediabetes N = 93	Diabetes N = 44	p-value ^a
LV EF (%)	70 (65;75)	70 (65;74)	72 (66;77)	69 (64;74)	0.03
LV EF <55%	14 (4.1%)	10 (4.8%)	0 (0%)	4 (9.1%)	0.01
LV myocardial mass (g)	141 (115;166)	127 (106;160)	151 (131;172)	148 (133;170)	<0.001
LV end-diastolic volume (ml m ⁻²)	66 (56;75)	69 (61;80)	60 (52;68)	55 (48;63)	<0.001
LVCI (g ml ⁻¹)	1.06 (0.9;1.28)	0.99 (0.87;1.14)	1.22 (1.02;1.35)	1.30 (1.05;1.57)	<0.001
LVCI >1.3 g ml ⁻¹	77 (22.3%)	26 (12.5%)	30 (32.3%)	21 (47.7%)	<0.001
LGE	8 (2.3%)	2 (1%)	4 (4.3%)	2 (4.6%)	0.06
LGE or LVCI >1.3 g ml ⁻¹ or LVEF <55%	93 (27%)	35 (16.8%)	33 (35.5%)	25 (56.8%)	<0.001

EF, ejection fraction; LGE, late gadolinium enhancement; LV, left ventricular; LVCI, left ventricular concentricity index.

Continuous data are expressed as median (interquartile range) and categorical data as number (percentage).

^a*p*-values derived from Kruskal-Wallis equality of population rank test (quantitative data), χ^2 -test (qualitative data) or Fisher's exact test (qualitative data).

Figure 4. Epi- and paracardial fat across normal glucose tolerance, prediabetes and diabetes. A stepwise increase was observed for both, epi- (A) and paracardial (B) fat (all $p < 0.001$).



In multivariate analysis, epicardial fat was strongly associated with VAT (β : 1.08, 95% CI: 0.76–1.40, $p < 0.001$) and weakly associated with current smoking ($p = 0.04$). Similarly, paracardial fat was also associated with VAT (β : 4.10, 95% CI: 3.32–4.88, $p < 0.001$; Table 5). All other associations to potential risk factors were dominated by the correlation to VAT.

Epi- and paracardial fat in the context of subclinical LV impairment

Both, epi- and paracardial fat were significantly higher in subjects with subclinical LV impairment as compared to subjects without impairment (Figure 5). Epicardial fat remained associated with LV impairment after adjustment for age, gender, smoking, hypertension, LDL and diabetes [β : 1.63 (0.5; 2.76), $p = 0.005$], but more importantly also including additional VAT [β : 1.13 (0.22; 2.03), $p = 0.02$]. Interestingly, the association attenuated in a model which included BMI instead of VAT ($p = 0.09$). For paracardial fat, the association to LV impairment was significant after adjustment for traditional risk factors [β : 4.92 (1.79; 8.05), $p = 0.002$], but became non-significant if the multivariate model included diabetes ($p = 0.13$) or any of the other obesity measures ($p = 0.47$ for the model including VAT and $p = 0.33$ for the model including BMI; Table 6).

DISCUSSION

In this study, we investigated cardiac fat depots as assessed by whole-body MRI in the context of impaired glucose metabolism and subclinical LV impairment. Although both, epi- and paracardial fat, were higher in subjects with impaired glucose tolerance, the association was largely confounded by traditional cardiovascular risk factors. In multivariate analysis, VAT was the strongest predictor for the amount of epi- and paracardial fat. Regarding the association to subclinical LV impairment, epicardial fat showed an independent association even after adjustment for traditional cardiovascular risk factors including VAT. In contrast, paracardial fat was not independently associated with subclinical LV impairment.

Body imaging, especially MRI with its benefit of no radiation exposure, has become an integral component in several epidemiological cohort studies including primarily healthy subjects, such as the German National Cohort or the UK Biobank aiming for 30,000 and 100,000 whole-body MR scans, respectively.²⁵ Thus, MR-based assessment of epicardial fat would potentially provide an important, imaging-based risk marker for cardiovascular disease. We found that manual assessment of the cardiac fat depots in the cine long-axis SSFP sequence (4-chamber view)

Table 3. Association of epicardial fat with impaired glucose metabolism

Epicardial fat	Normal glucose tolerance	Prediabetes		Diabetes	
		β (95 CI)	p -value	β (95 CI)	p -value
Unadjusted	-Ref.-	1.54 (0.23;2.84)	0.02	3.04 (1.39;4.68)	<0.001
Adjusted for					
Age, gender	-Ref.-	0.94 (-0.29;2.16)	0.14	1.98 (0.36;3.61)	0.02
Age, gender, CVRF	-Ref.-	0.55 (-0.66;1.76)	0.37	0.47 (-1.26;2.2)	0.59
Age, gender, CVRF, BMI	-Ref.-	0.3 (-0.87;1.47)	0.62	-0.08 (-1.71;1.56)	0.93
Age, gender, CVRF, SAT	-Ref.-	0.29 (-0.89;1.47)	0.63	0.35 (-1.3;2.01)	0.68
Age, gender, CVRF, VAT	-Ref.-	-0.41 (-1.55;0.73)	0.48	-0.92 (-2.53;0.7)	0.27

BMI, body mass index; CI, confidence interval; CVRF, cardiovascular risk factor; LDL, low-density lipoprotein; SAT, subcutaneous adipose tissue; VAT, visceral adipose tissue.

Bold font indicates significant p -values.

Stepwise adjustment including CVRF (hypertension, smoking, triglycerides, LDL), SAT and VAT.

Table 4. Association of paracardial fat with impaired glucose metabolism

Paracardial fat	Normal glucose tolerance	Prediabetes		Diabetes	
		β (95 CI)	<i>p</i> -value	β (95 CI)	<i>p</i> -value
Unadjusted	-Ref.-	5.15 (1.36;8.94)	0.01	13.08 (8.31;17.85)	<0.001
Adjusted for					
Age, gender	-Ref.-	4.45 (1.27;7.63)	0.01	8.77 (4.57;12.97)	<0.001
Age, gender, CVRF	-Ref.-	3.59 (-0.1;7.28)	0.06	5.43 (0.15;10.71)	0.04
Age, gender, CVRF, BMI	-Ref.-	1.77 (-1.34;4.88)	0.26	4.89 (0.54;9.24)	0.03
Age, gender, CVRF, SAT	-Ref.-	0.56 (-2.74;3.86)	0.74	4.68 (0.05;9.31)	0.048
Age, gender, CVRF, VAT	-Ref.-	-2.16 (-4.91;0.59)	0.12	-1.72 (-5.6;2.16)	0.39

BMI, body mass index; CI, confidence interval; CVRF, cardiovascular risk factor; LDL, low density lipoprotein; SAT, subcutaneous adipose tissue; VAT, visceral adipose tissue.

Bold font indicates significant *p*-values.

Stepwise adjustment including CVRFs (hypertension, smoking, triglycerides, LDL), SAT and VAT.

is feasible. Better reproducibility was observed for the systolic measurements, potentially due to better delineation of the fat depots. Teme et al found good correlations for end-systolic and end-diastolic epicardial fat volumes as assessed in SSFP short-axis in cardiac MRI.³⁵

Our research reflects previous findings that describe higher epicardial fat amounts in prediabetes¹⁸ and Type 2 diabetes.¹⁹ An early loss of significance for the association between epicardial fat and impaired glucose metabolism was observed. Our research is in line with a previous study conducted by Graeff et al who suggested that associations to cardiometabolic variables can be mainly explained—amongst others—by central obesity, in this respective study defined by waist circumference.²³ Interestingly,

paracardial fat was associated with diabetes even after adjustment for traditional cardiovascular risk factors. In an ultrasound vs MRI study, Sicari et al suggested paracardial fat to be a better cardiometabolic risk marker due to correlations of paracardial fat with, e.g. glucose, insulin sensitivity, BMI, blood pressure etc.¹⁵ However, the association in our study was finally confounded by VAT, thereby emphasizing the major role of VAT in metabolic disease, as has been outlined earlier.^{1,36} Beyond VAT, none of the other traditional cardiovascular risk factors showed an independent association with the cardiac fat depots, most likely due to shared pathophysiological pathways.

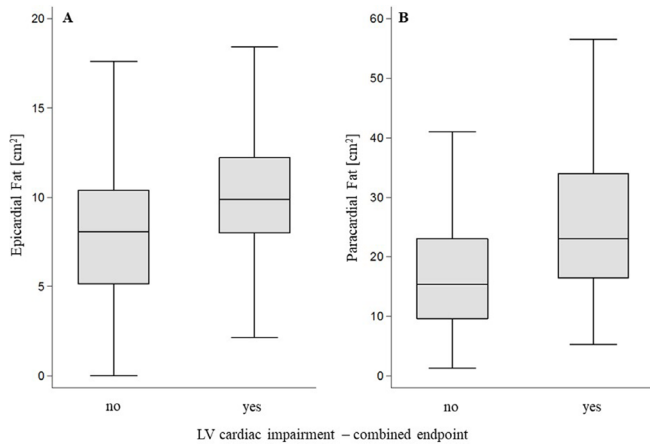
In our study, VAT was the strongest predictor for epicardial as well as paracardial fat in this clinically cardiovascular healthy

Table 5. Multivariable associations of cardiovascular risk factors including abdominal fat depots to epi- and paracardial fat

	Epicardial fat		Paracardial fat	
	β (95% CI)	<i>p</i> -value	β (95% CI)	<i>p</i> -value
Age (years)	0.03 (-0.03; 0.09)	0.27	0.01 (-0.14; 0.15)	0.93
Male gender (%)	-0.72 (-2.14; 0.70)	0.32	0.87 (-2.57; 4.31)	0.62
Hypertension (%)	-0.48 (-1.55; 0.59)	0.38	0.71 (-1.88; 3.31)	0.59
LDL (mg dl ⁻¹)	-0.01 (-0.03; 0.001)	0.08	0 (-0.04; 0.04)	1.00
HDL (mg dl ⁻¹)	0.004 (-0.03; 0.04)	0.81	0.005 (-0.08; 0.09)	0.91
Triglyceride (mg dl ⁻¹)	0.002 (-0.005; 0.008)	0.59	-0.002 (-0.02; 0.01)	0.8
Alcohol (g/day)	0.007 (-0.02; 0.03)	0.54	-0.03 (-0.08; 0.02)	0.29
Smoking				
Never-smoker	-Ref.-		-Ref.-	
Ex-smoker	0.8 (-0.23; 1.82)	0.13	-1.27 (-3.76; 1.23)	0.32
Current-smoker	1.39 (0.07; 2.70)	0.04	-1.45 (-4.64; 1.73)	0.37
VAT (l)	1.08 (0.76; 1.4)	<0.001	4.10 (3.32; 4.88)	<0.001
SAT (l)	-0.02 (-0.19; 0.16)	0.87	-0.46 (-0.89; -0.032)	0.04
PDFF _{hepatic} (%)	-0.04 (-0.11; 0.03)	0.21	-0.17 (-0.33; 0.001)	0.05

CI, confidence interval; HDL, high-density lipoprotein; LDL, low-density lipoprotein; PDFF, proton-density fat fraction; SAT, subcutaneous adipose tissue; VAT, visceral adipose tissue.

Figure 5. Epi- and paracardial fat between subjects with and without subclinical LV impairment. LV impairment was defined as a combined endpoint of LGE, EF <55% or LVCI >1.3 g ml⁻¹. Differences in both epi- (A) and paracardial (B) fat between the groups were significant ($p < 0.001$). EF, ejection fraction; LGE, late gadolinium enhancement; LV, left ventricular; LVCI, left ventricular concentricity index.



cohort. Our methodology in assessing epicardial fat differs from other cohort study set ups such as the Framingham Heart Study³ or the ELSA-Brasil study,²³ mainly due to the available imaging modality. In the Framingham Heart Study, CT-based volumetric assessment of epicardial fat was conducted³ while we analyzed epicardial fat on single slice measurements using a typical 4-chamber view. However, it was shown that there is overall good correlation for epicardial fat as measured by a single-slice area vs a volumetric approach.³⁷ In the ELSA-Brasil study, which showed that the association between epicardial fat thickness and cardiometabolic risk factors could be explained by age, gender, ethnicity and central obesity,²³ epicardial fat was assessed by echocardiography—a different imaging modality that only partially assesses epicardial fat. Another difference in many of these papers is the focus on the association between epicardial fat and cardiovascular disease, which is already clinically manifest^{3,38}—our approach analyses subclinical LV changes in a cohort without history of cardiovascular disease.

Our study suggests that epicardial fat is associated to MRI-derived markers of LV dysfunction. It needs to be taken into account that our study set up is cross-sectional and thus does not allow any conclusion regarding natural history of the disease and potential pathophysiological relationships. Nevertheless, in consideration together with other studies, which have analyzed the array of proinflammatory mediators in epicardial fat, *e.g.* in subjects undergoing coronary artery bypass surgery, and found elevated levels of pro-inflammatory mediators,^{5,6} the hypothesis of a local effect of epicardial fat on its neighboring structures such as the heart may be supported. Additionally, Cavalcante et al state that epicardial fat correlates independently with diastolic dysfunction.¹⁴ Furthermore, epicardial fat has been described as being associated with coronary artery stenosis and is increased in severe coronary artery calcification.³⁹ So far, vasocrine and paracrine signaling pathways have been suggested for communication between epicardial fat and its surrounding structures.^{40,41} However, further studies into the exact local pathomechanisms are warranted. Interestingly, the association in our study was not independent of BMI, a finding that may hint at the different role that the different fat depots play in the human body on different organ systems. This needs to be explored further in future studies.

Our results must be interpreted considering potential limitations. Overall, our study was not matched for age and gender. However, we adjusted for both age and gender in our multivariable models analyzing the associations between cardiac fat and diabetes status, as well as cardiac fat and LV impairment. By implication, the rest of our data needs to be regarded as descriptive information. Firstly, the study comprises only clinically cardiovascular healthy adults with Caucasian ethnicity. As it is known that the fat depots vary in different ethnicities,^{23,42} it remains unclear whether our findings have external validity in non-Caucasian cohorts. Also, we only studied subclinical alterations of the LV and did not include clinical outcomes nor measures of the left atrium, although epicardial fat has been shown to be associated to atrial fibrillation.¹² The manual segmentation of the cardiac fat depots may be a source of subjective error. Also, this approach may not be feasible in larger imaging cohorts as it is time-consuming and subjective, and further research into automated approaches that already exist for other fat depots³⁰ or other imaging modalities, is warranted.

Table 6. Multivariable association of epi- and paracardial fat to LV impairment

LV impairment	Epicardial fat		Paracardial fat	
	β (95 CI)	p -value	β (95 CI)	p -value
Unadjusted	1.80 (0.57; 3.03)	0.004	6.9 (3.3; 10.49)	<0.001
Adjusted for				
Age, gender, smoking, hypertension, LDL	1.26 (0.18; 2.35)	0.02	4.92 (1.79; 8.05)	0.002
Age, gender, smoking, hypertension, LDL, diabetes	1.63 (0.5; 2.76)	0.005	2.63 (-0.75; 6.00)	0.13
Age, gender, smoking, hypertension, LDL, diabetes, BMI	0.95 (-0.15; 2.05)	0.09	1.63 (-1.63; 4.89)	0.33
Age, gender, smoking, hypertension, LDL, diabetes, VAT	1.13 (0.22; 2.03)	0.02	0.88 (-1.53; 3.30)	0.47

BMI, body mass index; CI, confidence interval; LDL, low-density lipoprotein; LV, left ventricular; VAT, visceral adipose tissue.

LV impairment was defined as a combined endpoint of LGE, EF <55% or LVCI >1.3 g ml⁻¹. Bold font indicates significant p -values.

CONCLUSION

MRI-based assessment of epi- and paracardial fat in a study cohort setting is feasible, using the 4-chamber view, cine-SSFP sequence. Epi- but not paracardial fat is associated to subclinical LV impairment independent of traditional cardiovascular risk factors including VAT. Overall, VAT was the strongest predictor of both epicardial and paracardial fat in multivariate analysis, while differences between normal glucose tolerance, prediabetes and diabetes attenuated after adjustment.

FUNDING

The KORA study was initiated and financed by the Helmholtz Zentrum München – German Research Center for Environmental Health, which is funded by the German Federal Ministry of Education and Research (BMBF) and by the State of Bavaria. The MRT study was funded by the German Research Foundation (DFG, Bonn, Germany), the German Centre for Diabetes Research (DZD, Neuherberg, Germany) and the German Centre for Cardiovascular Disease Research (DZHK, Berlin, Germany).

REFERENCES

1. Fox CS, Massaro JM, Hoffmann U, Pou KM, Maurovich-Horvat P, Liu CY, et al. Abdominal visceral and subcutaneous adipose tissue compartments: association with metabolic risk factors in the Framingham Heart study. *Circulation* 2007; **116**: 39–48.
2. Abraham TM, Pedley A, Massaro JM, Hoffmann U, Fox CS. Association between visceral and subcutaneous adipose depots and incident cardiovascular disease risk factors. *Circulation* 2015; **132**: 1639–47. doi: <https://doi.org/10.1161/CIRCULATIONAHA.114.015000>
3. Mahabadi AA, Massaro JM, Rosito GA, Levy D, Murabito JM, Wolf PA, et al. Association of pericardial fat, intrathoracic fat, and visceral abdominal fat with cardiovascular disease burden: the Framingham Heart study. *European Heart Journal* 2009; **30**: 850–6. doi: <https://doi.org/10.1093/eurheartj/ehn573>
4. Rosito GA, Massaro JM, Hoffmann U, Ruberg FL, Mahabadi AA, Vasan RS, et al. Pericardial fat, visceral abdominal fat, cardiovascular disease risk factors, and vascular calcification in a community-based sample. *Circulation* 2008; **117**: 605–13. doi: <https://doi.org/10.1161/CIRCULATIONAHA.107.743062>
5. Baker A, da Silva N, Quinn D, Harte A, Pagano D, Bonser R, et al. Human epicardial adipose tissue expresses a pathogenic profile of adipocytokines in patients with cardiovascular disease. *Cardiovasc Diabetol* 2006; **5**: 1. doi: <https://doi.org/10.1186/1475-2840-5-1>
6. Mazurek T, Zhang L, Zalewski A, Mannion JD, Diehl JT, Arafat H, et al. Human epicardial adipose tissue is a source of inflammatory mediators. *Circulation* 2003; **108**: 2460–6. doi: <https://doi.org/10.1161/01.CIR.0000099542.57313.C5>
7. Marchington JM, Pond CM. Site-specific properties of pericardial and epicardial adipose tissue: the effects of insulin and high-fat feeding on lipogenesis and the incorporation of fatty acids in vitro. *Int J Obes* 1990; **14**: 1013–22.
8. Sacks HS, Fain JN, Holman B, Cheema P, Chary A, Parks F, et al. Uncoupling protein-1 and related messenger ribonucleic acids in human epicardial and other adipose tissues: epicardial fat functioning as brown fat. *J Clin Endocrinol Metab* 2009; **94**: 3611–5. doi: <https://doi.org/10.1210/jc.2009-0571>
9. Greulich S, Maxhera B, Vandenplas G, de Wiza DH, Smiris K, Mueller H, et al. Secretory products from epicardial adipose tissue of patients with type 2 diabetes mellitus induce cardiomyocyte dysfunction. *Circulation* 2012; **126**: 2324–34. doi: <https://doi.org/10.1161/CIRCULATIONAHA.111.039586>
10. Yerramasu A, Dey D, Venuraju S, Anand DV, Atwal S, Corder R, et al. Increased volume of epicardial fat is an independent risk factor for accelerated progression of sub-clinical coronary atherosclerosis. *Atherosclerosis* 2012; **220**: 223–30. doi: <https://doi.org/10.1016/j.atherosclerosis.2011.09.041>
11. Meenakshi K, Rajendran M, Srikumar S, Chidambaram S. Epicardial fat thickness: a surrogate marker of coronary artery disease – assessment by echocardiography. *Indian Heart Journal* 2016; **68**: 336–41. doi: <https://doi.org/10.1016/j.ihj.2015.08.005>
12. Thanassoulis G, Massaro JM, O'Donnell CJ, Hoffmann U, Levy D, Ellinor PT, et al. Pericardial fat is associated with prevalent atrial fibrillation: the Framingham Heart study. *Circ Arrhythm Electrophysiol* 2010; **3**: 345–50. doi: <https://doi.org/10.1161/CIRCEP.109.912055>
13. Iacobellis G, Zaki MC, Garcia D, Willens HJ. Epicardial fat in atrial fibrillation and heart failure. *Horm Metab Res* 2014; **46**: 587–90. doi: <https://doi.org/10.1055/s-0034-1367078>
14. Cavalcante JL, Tamarappoo BK, Hachamovitch R, Kwon DH, Alraies MC, Halliburton S, et al. Association of epicardial fat, hypertension, subclinical coronary artery disease, and metabolic syndrome with left ventricular diastolic dysfunction. *Amer J Cardiol* 2012; **110**: 1793–8. doi: <https://doi.org/10.1016/j.amjcard.2012.07.045>
15. Sicari R, Sironi AM, Petz R, Frassi F, Chubuchny V, De Marchi D, et al. Pericardial rather than epicardial fat is a cardiometabolic risk marker: an MRI vs echo study. *J Am Soc Echocardiogr* 2011; **24**: 1156–62. doi: <https://doi.org/10.1016/j.echo.2011.06.013>
16. Jung SH, Ha KH, Kim DJ. Visceral fat mass has stronger associations with diabetes and prediabetes than other anthropometric obesity indicators among Korean adults. *Yonsei Med J* 2016; **57**: 674–80. doi: <https://doi.org/10.3349/ymj.2016.57.3.674>
17. Neeland IJ, Turer AT, Ayers CR, Powell-Wiley TM, Vega GL, Farzaneh-Far R, et al. Dysfunctional adiposity and the risk of prediabetes and type 2 diabetes in obese adults. *JAMA* 2012; **308**: 1150–9. doi: <https://doi.org/10.1001/2012.jama.11132>
18. Arpacı D, Ugurlu BP, Aslan AN, Ersoy R, Akcay M, Cakir B. Epicardial fat thickness in patients with prediabetes and correlation with other cardiovascular risk markers. *Intern Med* 2015; **54**: 1009–14. doi: <https://doi.org/10.2169/internalmedicine.54.3714>
19. Song DK, Hong YS, Lee H, Oh JY, Sung YA, Kim Y. Increased epicardial adipose tissue thickness in type 2 diabetes mellitus and obesity. *Diabetes Metab J* 2015; **39**: 405–13. doi: <https://doi.org/10.4093/dmj.2015.39.5.405>
20. Bamberg F, Hetterich H, Rospleszcz S, Lorbeer R, Auweter SD, Schlett CL, et al. Subclinical disease burden as assessed by whole-body MRI in subjects with prediabetes, subjects with diabetes, and normal control subjects from the general population: the KORA-MRI study. *Diabetes* 2017; **66**: 158–69. doi: <https://doi.org/10.2337/db16-0630>
21. Devereux RB, Roman MJ, Paranicas M, O'Grady MJ, Lee ET, Welty TK, et al. Impact of diabetes on cardiac structure and function:

- the Strong Heart study. *Circulation* 2000; **101**: 2271–6.
22. Kannel WB, McGee DL. Diabetes and cardiovascular disease. The Framingham study. *JAMA* 1979; **241**: 2035–8.
 23. Graeff DB, Foppa M, Pires JC, Vigo A, Schmidt MI, Lotufo PA, et al. Epicardial fat thickness: distribution and association with diabetes mellitus, hypertension and the metabolic syndrome in the ELSA-Brasil study. *Int J Cardiovasc Imaging* 2016; **32**: 563–72. doi: <https://doi.org/10.1007/s10554-015-0810-z>
 24. Miao C, Chen S, Ding J, Liu K, Li D, Macedo R, et al. The association of pericardial fat with coronary artery plaque index at MR imaging: the multi-ethnic study of atherosclerosis (MESA). *Radiology* 2011; **261**: 11110346. doi: <https://doi.org/10.1148/radiol.11110346>
 25. Gatidis S, Heber SD, Storz C, Bamberg F. Population-based imaging biobanks as source of big data. *Radiol Med* 2017; **122**: 430–6. doi: <https://doi.org/10.1007/s11547-016-0684-8>
 26. Holle R, Happich M, Löwel H, Wichmann H, Group MKS. KORA - A Research Platform for Population Based Health Research. *Gesundheitswesen* 2005; **67**(Suppl 1): 19–25. doi: <https://doi.org/10.1055/s-2005-858235>
 27. World Health Organization, International Diabetes Federation. *Definition and diagnosis of diabetes mellitus and intermediate hyperglycaemia: report of a WHO/IDF consultation*. Geneva, Switzerland: World Health Organization; 2006.
 28. Seissler J, Feghelm N, Then C, Meisinger C, Herder C, Koenig W, et al. Vasoregulatory peptides pro-endothelin-1 and pro-adrenomedullin are associated with metabolic syndrome in the population-based KorA F4 study. *Eur J Endocrinol* 2012; **167**: 847–53. doi: <https://doi.org/10.1530/EJE-12-0472>
 29. Gaasch WH, Zile MR. Left ventricular structural remodeling in health and disease: with special emphasis on volume, mass, and geometry. *J Am Coll Cardiol* 2011; **58**: 1733–40. doi: <https://doi.org/10.1016/j.jacc.2011.07.022>
 30. Würslin C, Machann J, Rempp H, Claussen C, Yang B, Schick F. Topography mapping of whole body adipose tissue using a fully automated and standardized procedure. *J Magn Reson Imaging* 2010; **31**: 430–9. doi: <https://doi.org/10.1002/jmri.22036>
 31. Fallah F, Machann J, Martirosian P, Bamberg F, Schick F, Yang B. Comparison of T1-weighted 2D TSE, 3D SPGR, and two-point 3D Dixon MRI for automated segmentation of visceral adipose tissue at 3 tesla. *Magn Reson Mater Phys* 2017; **30**: 139–51. doi: <https://doi.org/10.1007/s10334-016-0588-6>
 32. Storz C, Heber SD, Rospleszcz S, Machann J, Sellner S, Nikolaou K, et al. The role of visceral and subcutaneous adipose tissue measurements and their ratio by magnetic resonance imaging in subjects with prediabetes, diabetes and healthy controls from a general population without cardiovascular disease. *Br J Radiol* 2018; **91**: 20170808. doi: <https://doi.org/10.1259/bjr.20170808>
 33. Hetterich H, Bayerl C, Peters A, Heier M, Linkohr B, Meisinger C, et al. Feasibility of a three-step magnetic resonance imaging approach for the assessment of hepatic steatosis in an asymptomatic study population. *Eur Radiol* 2016; **26**: 1895–904. doi: <https://doi.org/10.1007/s00330-015-3966-y>
 34. McGreevy KM, Lipsitz SR, Linder JA, Rimm E, Hoel DG. Using median regression to obtain adjusted estimates of central tendency for skewed laboratory and epidemiologic data. *Clin Chem* 2009; **55**: 165–9. doi: <https://doi.org/10.1373/clinchem.2008.106260>
 35. Teme T, Sayegh B, Syed M, Wilber D, Bakhos L, Rabbat M. Quantification of epicardial fat volume using cardiovascular magnetic resonance imaging. *J Cardiovasc Magn Reson* 2014; **16**(Suppl 1): O112. doi: <https://doi.org/10.1186/1532-429X-16-S1-O112>
 36. Lemieux S, Prud'homme D, Nadeau A, Tremblay A, Bouchard C, Despres JP. Seven-year changes in body fat and visceral adipose tissue in women. Association with indexes of plasma glucose-insulin homeostasis. *Diabetes Care* 1996; **19**: 983–91. doi: <https://doi.org/10.2337/diacare.19.9.983>
 37. Oyama N, Goto D, Ito YM, Ishimori N, Mimura R, Furumoto T, et al. Single-slice epicardial fat area measurement: do we need to measure the total epicardial fat volume? *Jpn J Radiol* 2011; **29**: 104–9. doi: <https://doi.org/10.1007/s11604-010-0524-z>
 38. Chen O, Sharma A, Ahmad I, Bourji N, Nestoiter K, Hua P, et al. Correlation between pericardial, mediastinal, and intrathoracic fat volumes with the presence and severity of coronary artery disease, metabolic syndrome, and cardiac risk factors. *Eur Heart J Cardiovasc Imaging* 2015; **16**: 37–46. doi: <https://doi.org/10.1093/ehjci/jeu145>
 39. Iwasaki K, Matsumoto T, Aono H, Furukawa H, Samukawa M. Relationship between epicardial fat measured by 64-multidetector computed tomography and coronary artery disease. *Clin Cardiol* 2011; **34**: 166–71. doi: <https://doi.org/10.1002/clc.20840>
 40. Yudkin JS, Eringa E, Stehouwer CDA. “Vasocrine” signalling from perivascular fat: a mechanism linking insulin resistance to vascular disease. *The Lancet* 2005; **365**: 1817–20. doi: [https://doi.org/10.1016/S0140-6736\(05\)66585-3](https://doi.org/10.1016/S0140-6736(05)66585-3)
 41. Sacks HS, Fain JN. Human epicardial adipose tissue: a review. *Am Heart J* 2007; **153**: 907–17. doi: <https://doi.org/10.1016/j.ahj.2007.03.019>
 42. Adams DB, Narayan O, Munnur RK, Cameron JD, Wong DT, Talman AH, et al. Ethnic differences in coronary plaque and epicardial fat volume quantified using computed tomography. *Int J Cardiovasc Imaging* 2017; **33**: 241–9. doi: <https://doi.org/10.1007/s10554-016-0982-1>